ELECTROCHEMICALLY ENHANCED DEPOSITION OF MINERALS FROM SYNTHETIC RESERVOIR BRINE

Laura Edvardsen*, Benjamin Udo Emmel, Mohammad Hossain Bhuiyan, Sigurd Wenner, Kamila Gawel, Malin Torsæter

SINTEF Industry, Trondheim, Norway

* Corresponding author e-mail: laura.edvardsen@sintef.no

Abstract

In this paper we ask the question whether or not electrochemically enhanced deposition of minerals can be utilized to repair leakage paths existing in cement plugs in wells. Electrical polarization of two electrodes may result in oxygen reduction and water electrolysis, where both processes change the local pH close to the two electrodes. The solution close to the anode is becoming acidic while close to the cathode it is becoming alkaline. Since solubility of many scaling minerals is pH dependent, precipitation of minerals on conductive surfaces can be induced by electrical polarization. We test whether cathodic polarization of conductive surfaces can be used to facilitate deposition of minerals from brines resembling reservoir fluids. As a model the reservoir formation water from the Gyda field was chosen. The electrochemically enhanced deposition at 23 and 120 °C from a synthetic Gyda brine was tested by polarizing at 5 V. The results show that cathodic polarization significantly enhanced precipitation of minerals from the synthetic Gyda brine.

Keywords: *electrochemical, mineralization, carbonates, well plugging*

1. Introduction

The Norwegian North Sea has an increasing amount of gas and oil fields that are depleted and shut down. These are candidates for storage of CO_2, and maybe in the future also hydrogen. The fields have a proven trapping and sealing capacity over geological timescales and might be suitable to guarantee safe storage of future renewable energy sources or CO_2. Until 2021, 24 gas and oil fields explored throughout the 1970 and 1980's have been shut down on the Norwegian continental margin [1]. Numerical studies and leakage incidents [2] indicate that wells are one of the major paths for gas (CH_4, CO_2, hydrogen) leakage [3].

At the end of the gas and oil production phase, wellbores are decommissioned *via* plugging and abandonment (P&A). To ensure that the P&A procedure seals the well and protects the surrounding (geological) environment against leakage in an eternal perspective, it is often necessary to remove long sections of steel pipes and create or repair annular barriers in the well. This is typically done by placing cement plugs inside the wells [4].

King et al. [5] compared statistics of well issues in the North Sea Norway, North Sea UK, and the Gulf of Mexico, and concluded that the major causes of well integrity issues were leakage through tubings and cement. The most probable leakage pathways via abandoned wells have been described by Gasda et al. [6]. One of them is a damaged cement plug. The sealing ability of the plugs can be impaired by chemical or mechanical degradation processes which may lead to gas leakage.

In this paper we suggest an electrochemical method for repairing cement plug damages and eliminating leakage pathways through these plugs.

The concept relies on utilizing cathodic polarization of the casing close to the cement plug (e.g., Figure 1 b), filled with scaling fluid to induce precipitation of minerals within or above the leakage pathway in order to plug (repair) it. The concept of anodic polarization of steel pipes has already been proposed for P&A purposes and the method has been tested for facilitation of pipe removal via enhanced corrosion. In contrast to its anodic counterpart, cathodic polarization protects steel pipes from corrosion. It has been shown that cathodic polarization of conductive surfaces in contact with scaling solution can lead to enhanced precipitation of scaling minerals like e.g., calcium carbonate [7]. Precipitation of scaling minerals is enhanced at high pH condition. Such conditions are induced in the vicinity of

electrode during cathodic polarization due to production of hydroxide ions, see Eq (1) [8].

$$2H_2O + 2e^- \rightarrow H_2 + 2OH^- \quad (1)$$

In this paper we test the concept of electrochemically enhanced deposition on a real scenario using formation water composition from the Gyda field sandstone reservoir. The electrochemically enhanced deposition at 23 and 120 °C from synthetic Gyda brine was tested. The reasons for choosing Gyda field for this case study is highlighted in Materials and Methods section.

2. Materials and method

2.1. Gyda case

The Gyda field (Figure 1.a) is in the southern part of the Norwegian North Sea, approximately 325 km southeast of Kristiansand. From 1990 to 2020 the field produced about 41 mill m^3 oil from a sandstone reservoir in the Ula formation at a depth of ca. 4000 m. The field temperature is around 155 °C and a high pressure of ca. 590 bar is prevailing. The claystone's of the Mandal formation provide a ca. 30 m thick seal. Six exploration wells and 53 production wells perforate the oil field with a well density of 1.44/km^2. In the discovery wellbore 2/1-3, hydrocarbons occur in three different formations in a depth ranging from ca. 3000 to 4100 m: (i) in the Tor formation limestone, (ii) in the Ula formation sandstone and (iii) in the Bryne formation sandstone [1].

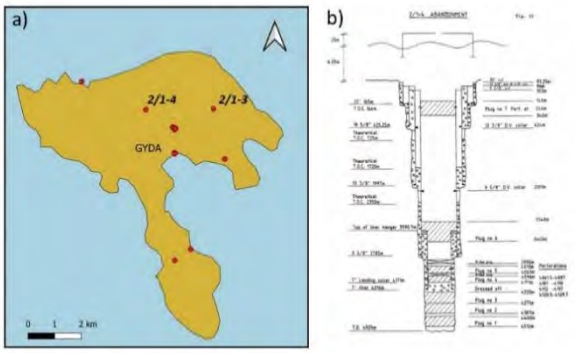

Figure 1. a) Extent of the Gyda filed (brown area) with wellbore locations (red dots). b) Example of an abandonment plan for exploration well 2/1-4 [1] indicating the depth of the build plugs (grey shaded area).

Gyda formation water composition (ionic composition, pH) was calculated as an average from six formation water samples reported by Warren et al. [9].

2.2 Preparation of synthetic Gyda formation water

Synthetic Gyda formation water (brine) was made by mixing the salts listed in Table 1 with deionized water for at least 1 hour. The solution is a simplified version of Gyda formation water reported in [9]. The initial solution is oversaturated at room temperature, thus some amount of salts remains precipitated.

Table 1. Ionic composition of synthetic and real Gyda formation water (fw) used for Phreeqc models. Salts (NaCl:130.57 g; $MgCl_2 \cdot 6H_20$: 17.65 g; KCl: 8.5 g $CaCl_2 \cdot 2H_20$: 97.42g; $NaHCO_3$: 0.6g; Na_2SO_4: 2.90 g and $FeCl_3$: 0.41 g) were mixed with deionized water to make up a total of 1 L solution.

	Synthetic Gyda fw	Real Gyda fw
Ion	**Mass (g/l)**	**Mass (g/l)**
Na^+	52.53	54.72
Mg^+	2.11	2.11
K^+	4.46	4.48
Ca^{2+}	26.56	26.51
Fe^{3+}	0.14	0.14
CO_3^{2-}	0.60	0.43
SO_4^{2-}	1.89	1.96
Cl^-	136.82	121.57
Ba^{2+}	-	0.32
Sr^{2+}	-	0.85

2.3 Geochemical modelling of pH and temperature changes

It is expected that local pH changes close to electrodes (polarized conductive surfaces) will lead to acceleration or inhibition of salt precipitation. To predict the impact of pH changes on the geochemical equilibrium between the Gyda brine and the precipitate, we modelled mineral dissolution/precipitation for different pH values and temperatures for the Gyda formation water with the composition described elsewhere [9]. The pressure, temperature and pH dependence of mineral reactions calculations have been done using the software Phreeqc with the *wateq4f.dat* data-base [10].

2.4 Electrochemical deposition

Electrochemical deposition was induced by applying a potential between two graphite electrodes immersed in an electrolyte (synthetic Gyda formation water). Graphite was chosen over metal to avoid corrosion of anode associated with the release of iron. Graphite tubes were used as cathode, anode and reference, and the potential between cathode and anode was set to 5 V. Experiments were conducted at 23 and 120 °C and the electrodes were polarized for 15 minutes. After the exposure, the electrodes were quickly flushed with deionized water to remove excess of brine and prevent excessive crystallization of the remaining salt during the drying process. Scanning electron microscopy (SEM) was used to investigate the topography of the electrode surfaces, and powder X-ray diffraction (XRD) was used to find the

mineralogical composition of the deposit. For SEM imagining of the surfaces, a Hitachi S3400 N thermal emission microscope was used with an acceleration voltage equal to 15 kV.

3. Results and discussions

3.1 Geochemical modelling

At first, we modelled the pH values that should be expected at different pressure/temperature conditions using the measured pH of the synthetic Gyda formation water (pH of 5.2 which is in line with the pH reported for Gyda brine samples [9]) as the initial value. The results in Figure 2 show the pH decrease from 5.2 to 4.7 with increasing temperature and pressure. The resulting data was further used as an input for geochemical modelling (Figure 3).

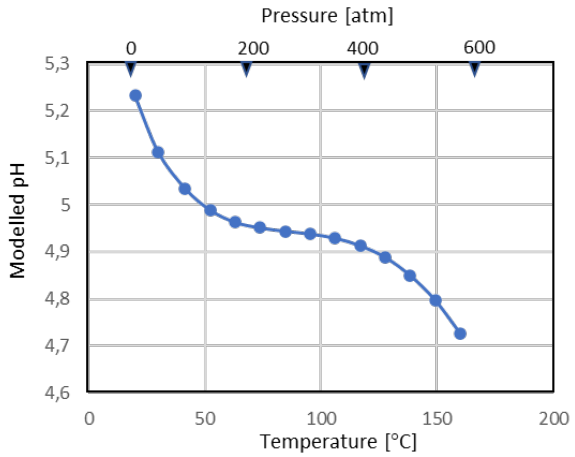

Figure 2. Modelled pH values for the Gyda formation water at different pressure/temperature conditions using Phreeqc. The initial conditions used were pH value of 5.2 at temperature of 23 ºC and 1 atm pressure.

Figure 3 shows modelled saturation indices (SI) for different model assumptions:

(i) Pressure/temperature and pH conditions at reservoir depth for the real and synthetic Gyda formation waters (T=154 °C; P=582 atm)

(ii) Pressure/temperature and pH conditions at laboratory conditions for the real and synthetic Gyda formation water (T=23 °C; P=1 atm)

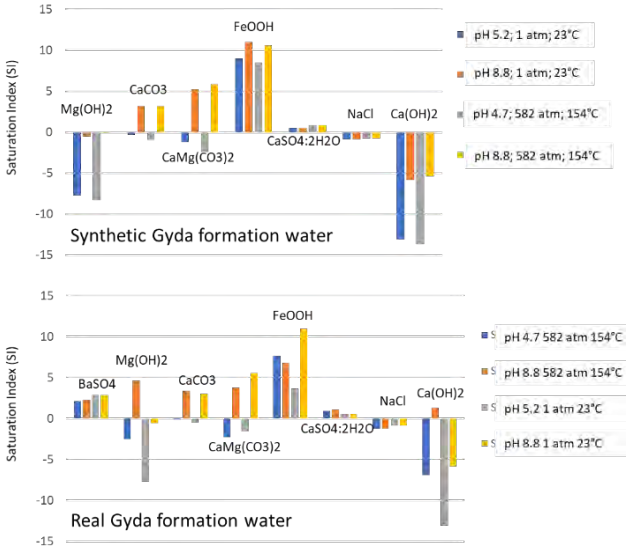

Figure 3. Saturation indices (SI) modelled for mineral phases at different pressure/temperature/pH conditions using the synthetic Gyda formation water (top) and real Gyda formation water (bottom) ionic composition.

A SI < 0 means the mineral phase is in the solution, and a SI > 0 means the solution is oversaturated and the phase will precipitate. From Figure 3 it is seen that the iron (Fe^{3+}) bearing phase (goethite) reach the highest saturation for all model assumptions. The main difference between synthetic and real Gyda formation water modelling was the presence of $BaSO_4$ in the real composition. Also, for the real composition, $Ca(OH)_2$ and $Mg(OH)_2$ have SI > 0 at pH 8.8, 582 atm and 154 °C, which is not the case for the synthetic composition.

Figure 4 shows modelled saturation indices at different pH values under laboratory conditions (room temperature and pressure) for the synthetic and real Gyda formation water. Only the Ca-bearing mineral phases and sodium chloride (NaCl) are presented.

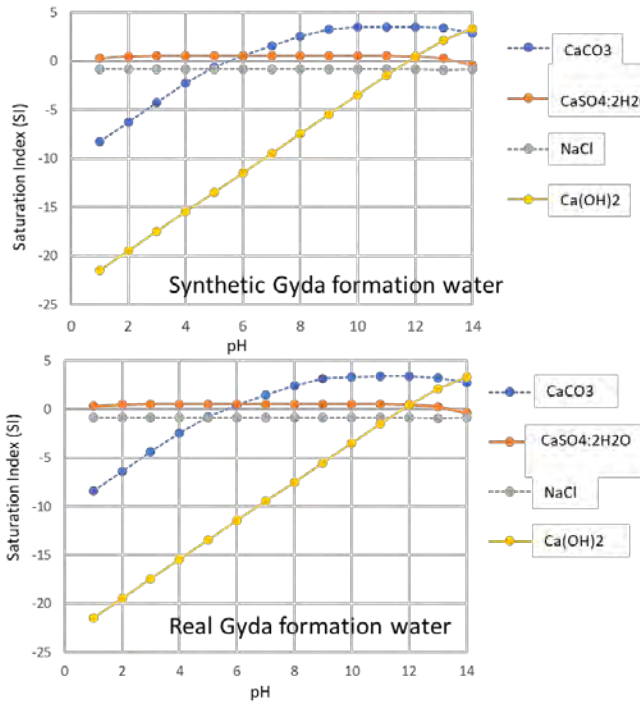

Figure 4. Modelled saturation indices (SI) for Ca-bearing mineral phases and NaCl at 23 °C, 1 atm for different pH values, using the synthetic Gyda formation water (top) and real Gyda formation water (bottom) ionic composition.

NaCl and gypsum ($CaSO_4 \cdot 4H_2O$) are relatively insensitive to pH variations. While NaCl had a SI lower than 0 for all pH values and would stay dissolved, $CaSO_4 \cdot 4H_2O$ precipitate at almost all pH values except from pH 14. At alkaline conditions (pH >12) portlandite ($Ca(OH)_2$) and calcium carbonate ($CaCO_3$) were shown to precipitate. If the pH close to the electrode is less than 12 but greater than 6, only $CaCO_3$ has a potential to precipitate.

3.2 Electrochemical deposition on graphite tubes

Figure 5 compares the surfaces of cathode, anode, and reference sample after only 15 minutes of polarization (5 V) in synthetic Gyda brine at different temperatures. The surfaces of the two cathode tubes were covered with a thick, white layer of minerals, while on the anode only a thin layer of precipitate was present. The precipitate on the anode occurred because the electrode stayed for 2 minutes in the brine solution after the potential was switched off, before the electrode was dismounted from the experimental setup and flushed with deionized water. The reference sample had a slightly thicker layer of precipitate than the anode. The large difference in amount of precipitate between the cathode and the reference sample indicates significant impact of electrical polarization on mineral deposition. It is thus suggested that the pH close to the cathode is larger than 6 at the experimental conditions (see Figure 4) as it accelerates precipitation. The local pH close to the cathode increases due to reduction of hydrogen and generation of hydroxide ions [11, 12]. On the contrary, the local pH close to the anode was acidic due to the production of hydrogen ions, which from Figure 4 is seen to inhibit precipitation of scaling minerals.

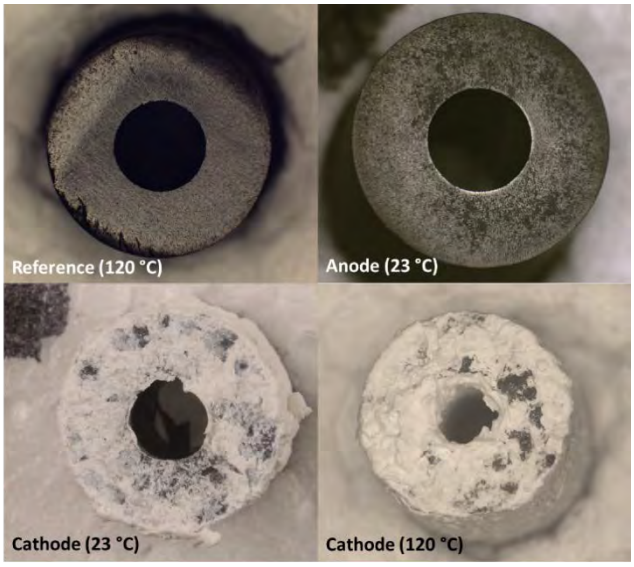

Figure 5. Photographs of graphite electrodes after 15 minutes of polarization at 5 V in synthetic Gyda formation water at 23 and 120 °C.

From Figure 5 it is also seen that an increase in temperature resulted in an increase of precipitate layer thickness on the cathode surface. This suggests that the temperature can further accelerate deposition processes.

Figure 6 presents SEM images showing the topography of precipitate deposited on the cathode surfaces after 15 minutes of polarization. Thick, partially cracked layers of precipitated material are present on both cathode surfaces.

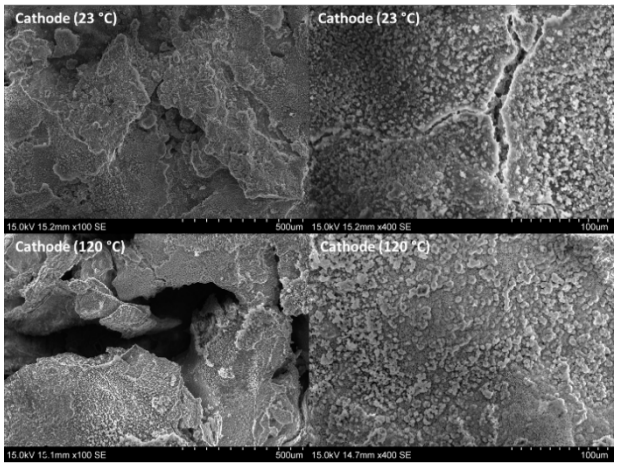

Figure 6. SEM images presenting topography of scale deposited at graphite surfaces after 15 minutes of polarization at 5 V in synthetic Gyda formation water.

X-ray powder diffraction patterns collected for the surface precipitates are presented in Figure 7. The patterns indicate the presence of peaks that are characteristic for portlandite ($Ca(OH)_2$), halite (NaCl) and calcite ($CaCO_3$). The major components found on the cathode surface were portlandite and halite, while calcite was only detected in relatively small quantities.

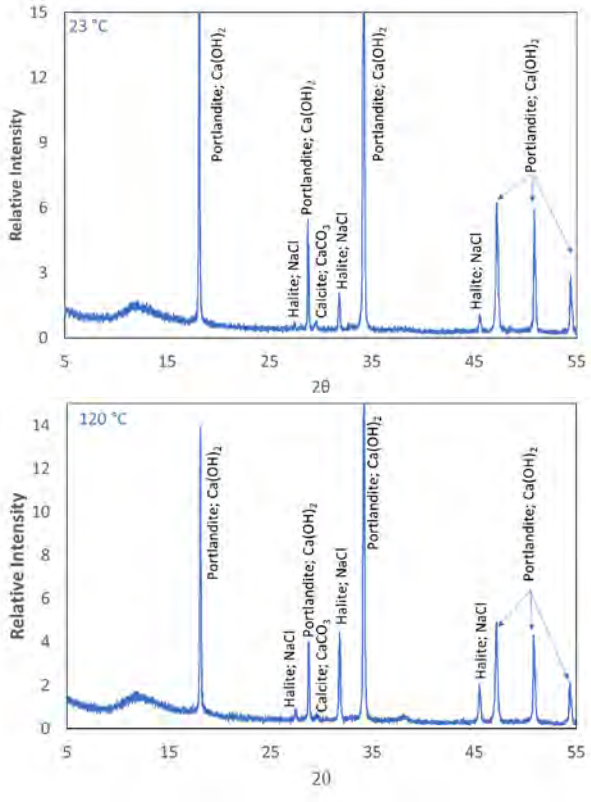

Figure 7. XRD patterns of material deposited at the surface of cathode polarized at 5 V at 23 and 120 °C. The peak characteristics for the different materials are ascribed.

Hydroxide ions are generated at the cathode, which increased the pH and promotes precipitation of portlandite through the following reaction [13]:

$$Ca^{2+} + 2OH^- \rightarrow Ca(OH)_2(s) \quad (2)$$

where the free Ca^{2+} ions come from dissolved $CaCl_2$ (see Table 1). The generation of hydroxide ions at the cathode also leads to an increased carbonate ion (CO_3^{2-}) concentration [14]. This promotes precipitation of calcite according to Eq (3) and (4),

$$HCO_3^- + OH^- \rightarrow CO_3^{2-} + H_2O \quad (3)$$

$$Ca^{2+} + HCO_3^- + OH^- \rightarrow CaCO_3(s) + H_2O \quad (4)$$

where the bicarbonate ions (HCO_3^-) originates from $NaHCO_3$. The scaling solution is only slightly undersaturated in respect to NaCl. It is thus likely that some small amounts of NaCl will co-precipitate along with portlandite due to e.g., locally changed concentration of sodium and chloride ions. Precipitation of calcite is known to increase with increasing temperature, but the effect of temperature is not as significant as the effect of pH [15]. The solubility of portlandite decrease with increasing temperature [16, 17] which explains the larger amount of precipitate at 120 °C compared to 23 °C. The presence of portlandite as the main mineral precipitated on the electrode surface together with the modelling results (Figure 4) suggest that the pH closest to the cathode surface was higher than 12.

3.3 Utilization of electrochemical deposition

Electrochemically enhanced mineral precipitation can be a method useful for future P&A, as well as maintenance of well integrity, to repairing plug damages and eliminate leakage pathways through cement plugs. However, utilization of electrochemical deposition in the context of CO_2 storage is highly dependent on the formation fluid. Brines needs to contain scaling ions like e.g., Ca^{2+}, Mg^{2+}, and carbonate and sulfate ions, which are common ions present in North Sea formation waters [9].

In this study, cathodic polarization of a graphite surface immersed in synthetic Gyda brine enhanced precipitation of portlandite. Portlandite is the main hydration product of Portland cement- a cement typically used for plugging of wells. It is expected that in contact with CO_2 brine the electrochemically precipitated portlandite could react to form calcium carbonate in a similar manner as portlandite present in cement material does [18, 19]. The reaction of portlandite with CO_2 is associated with volume increase which may additionally contribute to clogging of leakage pathways. A prerequisite to perform electrochemical clogging is good electrochemical communication between the cathode and the counter electrode. Achieving such a communication at downhole conditions may be the biggest challenge for the concept to be widely applicable.

4. Conclusions

In this paper we showed that cathodic and anodic polarization of conductive surfaces can be used to accelerate or inhibited scale deposition from reservoir brines rich in calcium like e.g., Gyda reservoir brine. Cathodic polarization at 5 V resulted in efficient precipitation of minerals from Gyda brine. The main minerals that precipitated were portlandite and smaller amounts of calcium carbonate. Increasing the temperature led to an increase in the amount of precipitate at the cathode surface. The acceleration and inhibition of scaling were driven by changes in the pH close to the electrode surfaces. Geochemical modelling

suggests that a pH value achieved at the electrode surface upon polarization at 5 V in the Gyda brine was above 12.

Acknowledgements

The authors gratefully acknowledge the financial support from The Norwegian Research Council in the form of grant number 285568 "Well fossilization for P&A" and from the strategic SINTEF Industry project number 102021203 "Electrophoretic cleaning and friction reduction for applications in drilling and well construction".

References

1. *Factpages Norwegian Petroleum Directorate - Gyda*. https://factpages.npd.no/en/field/PageView/ShutDown/43492.
2. Vielstädte, L., et al., *Quantification of methane emissions at abandoned gas wells in the Central North Sea.* Marine and Petroleum Geology, 2015. **68**: p. 848-860.
3. Alcalde, J., et al., *Estimating geological CO 2 storage security to deliver on climate mitigation.* Nature communications, 2018. **9**(1): p. 1-13.
4. Vrålstad, T., et al., *Plug & abandonment of offshore wells: Ensuring long-term well integrity and cost-efficiency.* Journal of Petroleum Science and Engineering, 2019. **173**: p. 478-491.
5. King, G.E. and D.E. King, *Environmental Risk Arising From Well-Construction Failure--Differences Between Barrier and Well Failure, and Estimates of Failure Frequency Across Common Well Types, Locations, and Well Age.* SPE Production & Operations, 2013. **28**(04): p. 323-344.
6. Gasda, S.E., S. Bachu, and M.A. Celia, *Spatial characterization of the location of potentially leaky wells penetrating a deep saline aquifer in a mature sedimentary basin.* Environmental geology, 2004. **46**(6-7): p. 707-720.
7. Edvardsen, L., et al., *Electrochemical enhancement and inhibition of calcium carbonate deposition.* Journal of Environmental Chemical Engineering, 2020. **8**(5): p. 104239.
8. Sheng, K., et al., *Formation and Inhibition of Calcium Carbonate Crystals under Cathodic Polarization Conditions.* Crystals, 2020. **10**(4): p. 275.
9. Warren, E.A., C.P. Smalley, and R. Howarth, *Part 4: compositional variations of North Sea formation waters.* Geological Society, London, Memoirs, 1994. **15**(1): p. 119-208.
10. Parkhurst, D.L. and C. Appelo, *Description of input and examples for PHREEQC version 3: a computer program for speciation, batch-reaction, one-dimensional transport, and inverse geochemical calculations*. 2013, US Geological Survey.
11. Persat, A., M.E. Suss, and J.G. Santiago, *Basic principles of electrolyte chemistry for microfluidic electrokinetics. Part II: Coupling between ion mobility, electrolysis, and acid–base equilibria.* Lab on a Chip, 2009. **9**(17): p. 2454-2469.
12. Kuhn, A. and C. Chan, *pH changes at near-electrode surfaces.* Journal of Applied Electrochemistry, 1983. **13**(2): p. 189-207.
13. Ellis, L.D., et al., *Toward electrochemical synthesis of cement—An electrolyzer-based process for decarbonating CaCO3 while producing useful gas streams.* Proceedings of the National Academy of Sciences, 2020. **117**(23): p. 12584-12591.
14. Chavez Panduro, E.A., et al., *Real time 3D observations of Portland Cement Carbonation at CO2 storage conditions.* Environmental science & technology, 2020. **54**(13): p. 8323-8332.
15. MacAdam, J. and S.A. Parsons, *Calcium carbonate scale formation and control.* Re/Views in Environmental Science & Bio/Technology, 2004. **3**(2): p. 159-169.
16. Justnes, H., et al., *Transformation kinetics of burnt lime in freshwater and sea water.* Materials, 2020. **13**(21): p. 4926.
17. Xinyu Zhang, F.P.G., K.L Scrivener, *Reaction kinetics of dolomite and portlandite.* Cement and Concrete Research, 2014. **66**: p. 11-18.
18. Tiong, M., R. Gholami, and M.E. Rahman, *Cement degradation in CO 2 storage sites: a review on potential applications of nanomaterials.* Journal of Petroleum Exploration and Production Technology, 2019. **9**(1): p. 329-340.
19. Kutchko, B.G., et al., *Degradation of well cement by CO2 under geologic sequestration conditions.* Environmental science & technology, 2007. **41**(13): p. 4787-4792.